

Numerical study on buckling of steel web plates with openings

Mohammed H. Serror^{*}, Ahmed N. Hamed^a and Sherif A. Mourad^b

Department of Structural Engineering, Faculty of Engineering, Cairo University, Egypt

(Received July 25, 2016, Revised November 25, 2016, Accepted December 01, 2016)

Abstract. Cellular and castellated steel beams are used to obtain higher stiffness and bending capacity using the same weight of steel. In addition, the beam openings may be used as a pass for different mechanical fixtures such as ducts and pipes. The aim of this study is to investigate the effect of different parameters on both elastic and inelastic critical buckling stresses of steel web plates with openings. These parameters are plate aspect ratio; opening shape (circular or rectangular); end distance to the first opening; opening spacing; opening size; plate slenderness ratio; steel grade; and initial web imperfection. The web/flange interaction has been simplified by web edge restraints representing simply supported boundary conditions. A numerical parametric study has been performed through linear and nonlinear finite element (FE) models, where the FE results have been verified against both experimental and numerical results in the literature. The web plates are subject to in-plane linearly varying compression with different loading patterns, ranging from uniform compression to pure bending. A buckling stress modification factor (β -factor) has been introduced as a ratio of buckling stress of web plate with openings to buckling stress of the corresponding solid web plate. The variation of β -factor against the aforementioned parameters has been reported. Furthermore, the critical plate slenderness ratio separating elastic buckling and yielding has been identified and discussed for two steel grades of DIN-17100, namely: ST-37/2 and ST-52/3. The FE results revealed that the minimum β -factor is 0.9 for web plates under uniform compression and 0.7 for those under both compression and tension.

Keywords: numerical study; web plate with openings; elastic and inelastic buckling; buckling stress modification factor

1. Introduction

Unlike longitudinal members such as columns, plates are able to continue carrying loads after buckling in a stable manner. The post-buckling strength can be substantially greater than the corresponding buckling strength. This structural property is of great interest to structural engineers. Both numerical and experimental investigations were performed over the past decades to study the buckling behavior of steel plates with and without openings under different loading and boundary conditions (Narayanan and Chow 1984, Thomas 1996, Bruneau *et al.* 1998, Shanmugam *et al.* 1999, El-Sawy and Nazmy 2001, El-Sawy *et al.* 2004, Komur and Sonmez 2008, Maiorana *et al.* 2009, Sweedan and El-Sawy 2011 and Kang 2014).

Approximate methods, with charts suitable for the use of designers, were developed to predict

^{*}Corresponding author, Associate Professor, E-mail: serror@eng.cu.edu.eg

^aGraduate Student

^bProfessor

the ultimate load capacity of square simply supported plates with central circular and square openings (Narayanan and Chow 1984). Design formulas were also proposed based on regression analysis for FE results to evaluate the plate ultimate load capacity (Shanmugam *et al.* 1999) and the plate buckling coefficient (K) (Maiorana *et al.* 2009) against opening size, orientation, and location, and plate aspect ratio under the combined effect of compression and bending. Moreover, closed-form expressions were developed to approximate the influence of single and multiple openings on the critical elastic buckling stress for rectangular plates subject to compression or bending (Moen and Shafer 2009).

Openings can either decrease or increase the plate critical elastic buckling stress depending on the opening geometry and spacing. Rectangular openings with curved corners were studied, and recommendations were given for the size and location of openings to enhance elastic stability of the perforated plates (El-Sawy and Nazmy 2001). Both elastic and inelastic buckling stresses were obtained in association with the plate slenderness ratio for different steel grades (El-Sawy *et al.* 2004). Furthermore, it was recommended that the center of the single circular cutoff should not be placed in the outer half of the end panel of a rectangular plate (Komur and Sonmez 2008). It is worth noting that the web/flange interaction was simplified in the aforementioned studies by plate edge restraint, where results revealed limits on opening geometry and spacing to improve the plate stability (Sweedan and El-Sawy 2011).

Design methods were proposed for steel I-shaped beams with circular web openings (Chung *et al.* 2001, and Panedpojaman and Rongram 2014), considering shear yielding and moment-shear interaction at the opening location. The ultimate load capacity was assumed limited by the formation of plastic hinges at the top tee-section at the web opening location. In addition, FE models were established to predict the behavior and the ultimate load capacity of steel I-shaped beams with web openings (Shanmugam *et al.* 2002). The contribution of web slenderness and flange stiffness was considered in the investigation. On the other hand, FE models were developed to study the effect of a single rectangular web opening on lateral torsional buckling and local buckling of simply supported steel I-shaped beams subject to uniform bending (Serror 2011). Regression analysis was performed on the FE results to develop a mathematical expression for the resulted reduction in beam bending capacity. It was reported that the web opening might change the mode of beam buckling from lateral torsional buckling to local buckling but not the reverse. In addition, it was recommended to use web opening with a height that is less than half of the beam height, to have a limited reduction in beam bending capacity. The numerical results were compared with those obtained by design methods presented in design codes (Soltani *et al.* 2012).

Experimental and numerical studies were conducted on cellular and castellated steel beams with circular, square, rectangular, hexagonal and octagonal web openings subject to different loading and boundary conditions (Redwood *et al.* 1996, Tsavdaridis and Mello 2011, Anghel *et al.* 2011, Ellobody 2012, Kamble 2012, Soltani *et al.* 2012, Wakchaure *et al.* 2012, Durif *et al.* 2014, and Wang *et al.* 2014). Strain and deflection were measured near the most critical openings, and a profile of lateral web deflections was obtained at the critical web posts (Redwood *et al.* 1996). It was reported that adding web stiffeners, connecting the tension flange to the compression flange, enhances the lateral buckling behavior of I-shaped beams with web openings (Anghel *et al.* 2011). It was also reported that the presence of web distortional buckling causes a considerable decrease in the failure load. Furthermore, the investigation results revealed that the use of high strength steel offers a considerable increase in the failure loads of less slender castellated steel beams (Ellobody 2012). Meanwhile, the use of beams with openings is efficient for moderately loaded long spans where the design is controlled by deflection (Wakchaure *et al.* 2012). The vierendeel

failure mechanism of castellated steel beams with fillet corners of web openings was investigated (Wang *et al.* 2014). The results revealed that beams with fillet corners of web openings have higher load capacity than those with rectangular or hexagonal openings. A design optimization problem was developed, where the optimization solution was carried out such that the design limitations are satisfied and the weight of the beam is the minimum (Erdal *et al.* 2011). The design algorithms recommended optimum opening diameter and optimum number of openings in the beam. The buckling behavior of axially loaded steel I-shaped columns with web openings was also investigated (El-Sawy *et al.* 2009, Sonck *et al.* 2011, 2014 and Yuan *et al.* 2014). The FE results were employed to identify dimensionless modification factors for the buckling load and the equivalent section properties.

In this numerical study, linear and nonlinear FE analyses have been performed to investigate the effect of different parameters on both elastic and inelastic critical buckling stresses of steel web plates with openings. The plates are subject to in plane linearly varying compression with different loading patterns, ranging from uniform compression to pure bending. The parameters in question are plate aspect ratio; opening shape (circular or rectangular); end distance to first opening; opening spacing; opening size; plate slenderness ratio; steel grade; and initial web imperfection. The web/flange interaction has been simplified by rotation-free edge restraints, representing the critical boundary conditions.

2. Numerical model

The numerical model is based on the finite element method (FEM), where models for web plate with openings have been established using the general-purpose FEM software ANSYS (1998). The four-node shell element “shell-181” has been employed. This element has 6 degrees of freedom at each node and is well suited for linear, large rotation, and large strain nonlinear applications. The most suitable element size has been determined by conducting a mesh sensitivity analysis using the h-refinement procedure at which the size of the element has been progressively reduced until convergence. The mesh sensitivity analysis has been performed for both the solid and the perforated plate models. The selected mesh has been verified by comparing the obtained FE elastic buckling load with the closed-form solution and the experimental results published in the literature.

To assess the elastic buckling load and the inelastic ultimate load of web plates with openings subject to uniaxial compression, two-dimensional FE models have been established. The inelastic buckling analysis accounts for both material and geometric nonlinearities. Hence, initial geometric imperfection has been assumed equal to [plate height/10,000] having the shape of the fundamental buckling mode. The Arc-length method with large deformations has been adopted to trace the relation between load value and out of plane deformation taking into account both material and geometric nonlinearities. The analysis has been set to terminate at first limiting point when the material reaches Von Mises yield stress.

For the elastic buckling analysis, a linear elastic material has been employed with $E = 210$ GPa (elasticity modulus) and $\nu = 0.33$ (Poisson's ratio). For the inelastic buckling analysis, the material has been modeled with elastic-perfectly plastic stress-strain behavior, where E and ν are same as those of the elastic material. Two steel materials have been considered, namely: DIN-17100 ST-37/2 with $F_y = 240$ MPa (yield stress) and $F_u = 360$ MPa (tensile stress); and DIN-17100 ST-52/3 with $F_y = 360$ MPa (yield stress) and $F_u = 520$ MPa (tensile stress). In general, the material has

been assumed to be homogenous, isotropic and rate independent.

Fig. 1(a) illustrates two main geometrical models that have been established: one for circular openings with diameter (D) and the other for square openings with side length (a). The web plate has length (L), height (h_w) and thickness (t_w). The opening has end distance (e), and equal spacing (S). The characteristics of the geometric models have been listed in Table 1. Fig. 1(b) illustrates the loading patterns that have been applied to the web plate. Linearly varying stress pattern has been applied to the plate ends, as shown in Fig. 1(d). The stress pattern is identified by stress ratio (ψ) which is defined as the ratio between top and bottom end stresses, where $\psi = 1.0$ represents uniform compression and $\psi = -1.0$ represents pure bending moment. Five different patterns have been adopted in this study ($\psi = 1.0, 0.5, 0.0, -0.5, \text{ and } -1.0$) to simulate different web loading conditions in beam, column, and beam-column members (Kang 2014), as shown in Fig. 1(b). The loading patterns range from uniform compression to pure bending.

The buckling has been observed at three different locations within the web plate, namely: (1) at the plate end strip that is formed at the plate end opening; (2) at the plate post strip that is formed in between plate openings; and (3) at the plate longitudinal strips that are formed above and below plate openings. The three locations have been illustrated in Fig. 1(c). Fig. 1(d) illustrates the applied displacement boundary conditions to the web plate. The top and bottom edges of the plate may have rotation restraint ($R_x = R_y = 0$) to represent the effect of a beam flange with high stiffness relative to the web (preventing rotation of web plate at the edges). On the other hand, they may have rotation-free condition to represent the effect of a beam flange with lower stiffness that cannot restrain the web plate rotation at the edges. The critical case of rotation-free at the top and bottom edges of the web plate has been adopted in this study (Thomas 1996, Shanmugam *et al.* 1999). The out of plane translation in Z direction (U_z) has been restrained along web plate perimeter. The translation in X direction (U_x) has been restrained at all nodes along the line of geometrical symmetry. In order to prevent the rigid body motion of the plate, the translation in Y direction (U_y) has been restrained at two symmetrical nodes, at the start and end of the plate along the horizontal centerline. It is worth noting that the symmetrical model shown in Fig. 1(d) has been adopted for inelastic buckling analysis in order to reduce the analysis time.

For the elastic buckling study, a buckling stress modification factor (β -factor) has been defined as a ratio of buckling stress of web plate with openings to buckling stress of the corresponding solid plate. Hence, β -factor equals ($\beta = K_c/K_{\text{solid}}$), where K_c and K_{solid} are the elastic buckling coefficients for the plate with openings and the solid plate, respectively. On the other hand for inelastic buckling study, a stress ratio (σ_{cr}/σ_y) has been defined, where σ_{cr} and σ_y are the inelastic critical buckling stress and the yield stress, respectively. The variation of both β -factor and (σ_{cr}/σ_y) ratio with different geometric parameters has been depicted.

Table 1 Numerical model parameters and range of study

Parameter	Range of study
L/h_w	10 to 30
h_w/t_w	30 to 150
e	$0.5h_w$ to $2.5h_w$
S	$1.0h_w$ to $3.0h_w$
$D, a, \text{ and } b$	$0.4h_w$ to $0.8h_w$
Imperfection	$h_w/200, h_w/150, \text{ and } h_w/100$

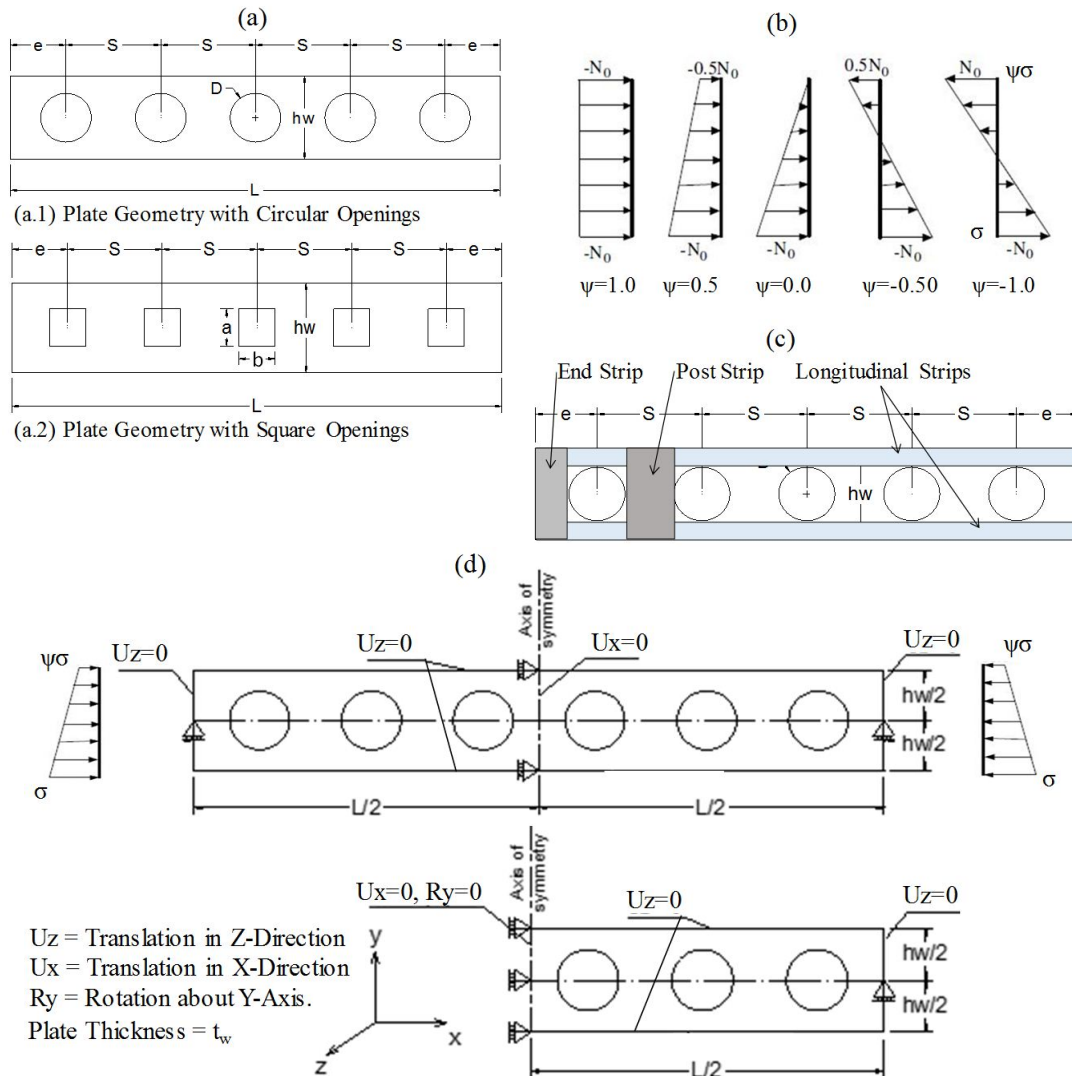


Fig. 1 Web plate model: (a) geometry; (b) loading patterns; (c) anticipated buckling locations; and (d) applied boundary conditions

3. Numerical model verifications

3.1 Verification-1: FE model mesh size

Fig. 2 demonstrates the verification models that have been generated for a simply supported steel plate of $3000 \times 600 \times 10$ (length \times height \times thickness in mm) to verify the proper FE mesh size. Elastic buckling analysis has been performed in ANSYS under three patterns of in plane uniaxial compression ($\psi = 1.0, 0.0$ and -1.0), as shown in Fig. 2(a). Mesh sensitivity analysis has been carried out by using the h-refinement procedure at which the mesh size is progressively reduced, for each load pattern, until a converged solution is reached. The convergence of resulted

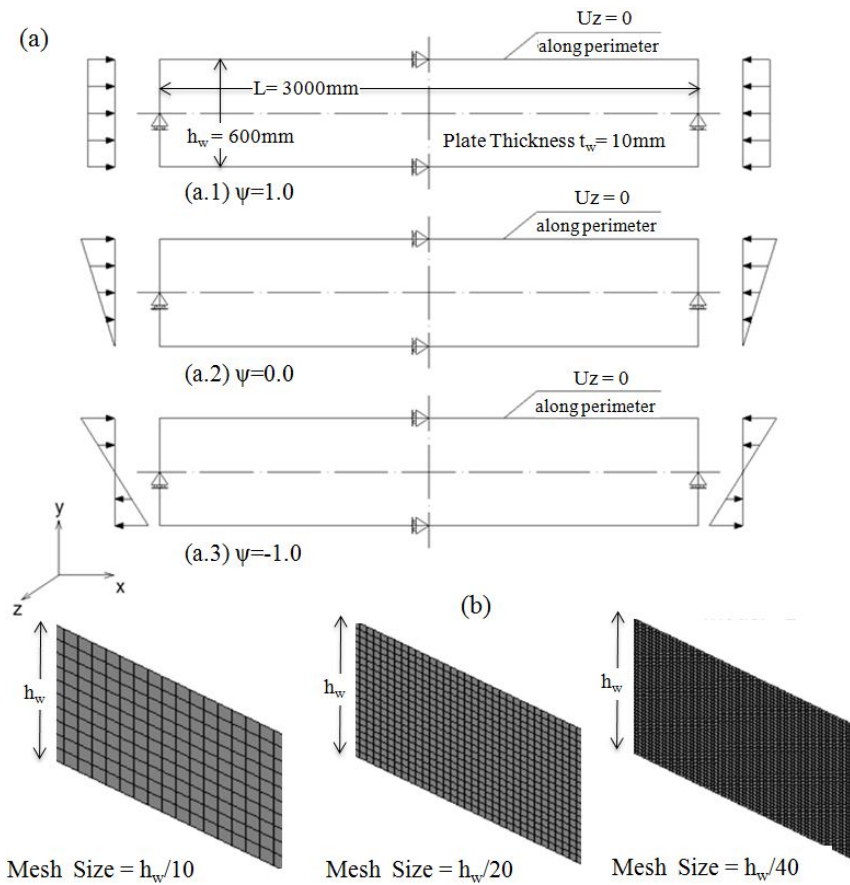


Fig. 2 Verification-1 Models

Table 2 Verification-1 results ($\sigma_{cr_Numerical}$) against closed-form solution (σ_T) by Timoshenko and Gere (1961)

Mesh size	Loading pattern								
	$\psi = 1.0$			$\psi = 0.0$			$\psi = -1.0$		
	$\sigma_{cr_Numerical}$ (MPa)	σ_T (MPa)	Error (%)	$\sigma_{cr_Numerical}$ (MPa)	σ_T (MPa)	Error (%)	$\sigma_{cr_Numerical}$ (MPa)	σ_T (MPa)	Error (%)
$h_w/10$	2.097	2.109	0.569	4.095	4.106	0.268	12.47	12.602	1.047
$h_w/20$	2.106	2.109	0.142	4.112	4.106	0.146	12.59	12.602	0.095
$h_w/40$	2.108	2.109	0.047	4.107	4.106	0.024	12.61	12.602	0.063

buckling stress has been compared with the closed-form solution by Timoshenko and Gere (1961). Fig. 2(b) shows the progressively reduced mesh size from ($h_w/10$) to ($h_w/40$). Table 2 lists the resulted elastic buckling stress (σ_{cr}) against the closed-form solution by Timoshenko and Gere (1961) (σ_T) for each mesh size and loading pattern. It is evident that the accuracy of the numerical solution has been progressively improved with the reduction in mesh size. Accordingly, a mesh size of ($h_w/40$) has been adopted in this study.

3.2 Verification-2: Elastic buckling of plate with central opening

Elastic buckling analysis has been performed in ANSYS for a simply supported steel plate with central opening under uniaxial uniform compression, as shown in Fig. 3. The generated numerical models simulate specimens that have been tested in the experimental work by Narayanan and Chow (1984) and the numerical work by El-Sawy and Nazmy (2001). Both circular and square openings have been considered, and a FE mesh size of $(h_w/40)$ has been adopted. Table 3 lists the resulted numerical buckling load that is in good agreement with the reported load in the experimental work. Furthermore, the resulted buckling coefficient (K) has been compared with that reported by El-Sawy and Nazmy (2001), where it is evident in Fig. 4 that both results are in full match.

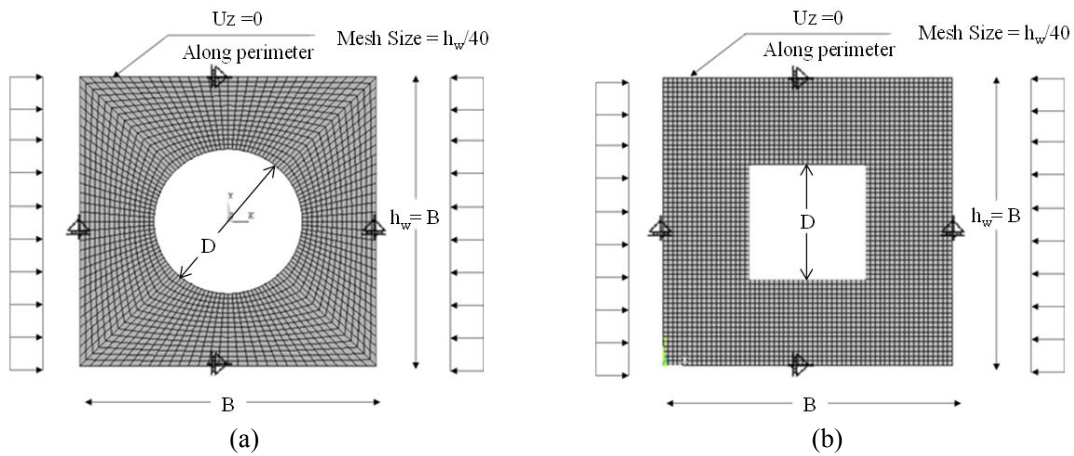


Fig. 3 Verification-2 Models

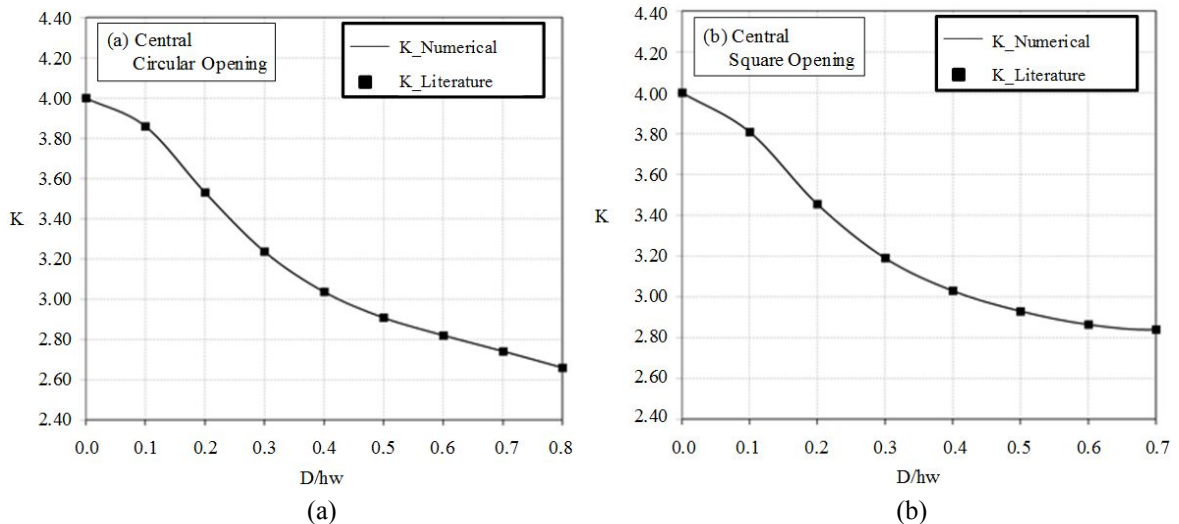


Fig. 4 Verification-2 numerical results ($K_{\text{Numerical}}$) against literature results ($K_{\text{Literature}}$) by El-Sawy and Nazmy (2001)

Table 3 Verification-2 results ($P_{\text{Numerical}}$) against experimental work results ($P_{\text{Experimental}}$) by Narayanan and Chow (1984)

Specimen ID	D/B	$P_{\text{Numerical}}$ (kN)	$P_{\text{Experimental}}$ (kN)	Error (%)
PL1	0	24.988	25.064	0.303
CIR2a	0.2	21.960	22.504	2.417
CIR3a	0.3	20.154	21.311	5.429
CIR4a	0.4	18.921	19.706	3.983
CIR5a	0.5	18.140	19.482	6.888
SQ2	0.2	21.550	22.600	4.646
SQ3	0.3	19.907	20.290	1.888
SQ4	0.4	18.907	18.230	3.714
SQ5	0.5	18.282	19.170	4.632

3.3 Verification-3: Elastic buckling of plate with openings

The numerical model for plate with multiple openings has been verified against the work performed by Sweedan and El-Sawy (2011). The plates have been tested under linearly varying uniaxial compression. The loading and displacement boundary conditions shown in Fig. 1 have been applied; in addition, a mesh size of $h_w/40$ has been adopted. Table 4 shows a comparison between results reported by Sweedan and El-Sawy (2011) and those obtained by the numerical model. The index parameter is set to be the buckling load modification factor (β) due to the introduction of plate openings. It is evident that the results are in good agreement.

Table 4 Verification-3 results ($\beta_{\text{Numerical}}$) against literature work results ($\beta_{\text{Literature}}$) by Sweedan and El-Sawy (2011)

L/h_w	S/D	D/h_w	$\psi = 1.0$			$\psi = -1.0$		
			$\beta_{\text{Numerical}}$	$\beta_{\text{Literature}}$	Error (%)	$\beta_{\text{Numerical}}$	$\beta_{\text{Literature}}$	Error (%)
10	1.25	0.4	0.795	0.800	0.625	0.600	0.600	0.000
		0.8	0.652	0.650	0.308	0.991	0.990	0.101
	5	0.4	0.971	0.975	0.410	0.828	0.825	0.364
		0.8	1.050	1.050	0.000	1.025	1.025	0.000

3.4 Verification-4: Inelastic buckling of plate with central opening

Inelastic buckling analysis has been performed for a simply supported square plate with central circular opening under in plane uniaxial uniform compression to simulate the test model analyzed by Shanmugam *et al.* (1999). The model geometry, loading and boundary conditions are similar to that presented in Fig. 3(a). Elastic perfectly plastic material model has been adopted applying Von-Mises yield criteria. The steel used has a yield stress (σ_y) that is equal to 360 MPa. Geometric imperfection has been introduced in alignment with the fundamental mode shape of buckling deformation. The amplitude of imperfection has been chosen to be equal to $h_w/2000$ after trials of

different values to obtain matching results. This imperfection amplitude is considered to represent the case of perfect plate since the maximum permitted out-of-flatness is as big as $h_w/120$ and $h_w/150$ according to AASHTO (1994) and AWS-D1.1 (2004), respectively. The loading has been applied in increments and equilibrium equations have been solved using the modified Newton-Raphson technique. The load increments have been determined by the Arc-Length method, and the analysis has been terminated as soon as the limit load is reached.

Table 5 lists a comparison between results reported by Shanmugam *et al.* (1999) and those obtained by the numerical model. Different values of plate slenderness ratio (h_w/t_w) and normalized opening size (D/h_w) have been considered, where the comparison revealed good agreement between the results.

Table 5 Verification-4 results ($\sigma_{CR_Numerical}/\sigma_y$) against literature work results ($\sigma_{CR_Literature}/\sigma_y$) by Shanmugam *et al.* (1999)

h_w/t_w	$D/h_w = 0.1$			$D/h_w = 0.2$			$D/h_w = 0.3$		
	$\sigma_{CR_Numerical} / \sigma_y$	$\sigma_{CR_Literature} / \sigma_y$	Error (%)	$\sigma_{CR_Numerical} / \sigma_y$	$\sigma_{CR_Literature} / \sigma_y$	Error (%)	$\sigma_{CR_Numerical} / \sigma_y$	$\sigma_{CR_Literature} / \sigma_y$	Error (%)
30	0.917	0.910	0.769	0.812	0.810	0.247	0.718	0.710	1.127
40	0.890	0.860	3.488	0.795	0.790	0.633	0.697	0.690	1.014
50	0.767	0.760	0.921	0.696	0.720	3.333	0.623	0.640	2.656

4. Results and discussion

4.1 Elastic buckling

Fig. 5 illustrates the variation of buckling stress modification factor (β -factor) versus plate aspect ratio (L/h_w) for various values of opening end distance (e), spacing (S), and size (“ D ” for circular opening, or “ a ” for square opening). The behavior has been depicted under both uniform compression and pure bending. It is evident that, in all cases, the plate aspect ratio has no effect on the β -factor. Figs. 6-10 illustrate the variation of buckling stress modification factor (β -factor) versus opening end distance for various values of opening spacing and size. Figs. 6-8 are dedicated for plates with circular openings; meanwhile, Figs. 9 and 10 are dedicated for those with square openings. The behavior has been reported, hereafter, under different loading patterns ranging from uniform compression to pure bending. When β -factor approaches 1.0, it implies that the buckling behavior of web plate with openings is identical to that of the corresponding solid plate. When β -factor is greater than 1.0, it implies that the buckling behavior of web plate with openings is superior to that of the corresponding solid plate. Thus, when β -factor is less than 1.0, it implies that the buckling behavior of web plate with openings is badly affected by the introduction of openings compared with the corresponding solid plate.

For web plate with openings subject to compression loading ($\psi = 1.0, 0.5, \text{ and } 0.0$), the following observations have been detected. At end distance less than or equal to a first limiting value ($e_{Limit-1}$), the plate end strip suffers buckling at a stress value less than those at longitudinal and post strips buckling (as shown in Fig. 11(a1)). Thus, when opening size increases the end strip width decreases (width = $[e-D/2]$ for circular opening, or $[e-a/2]$ for square opening), leading to a lower buckling stress. This is the reason behind the reported adverse relation between β -factor and

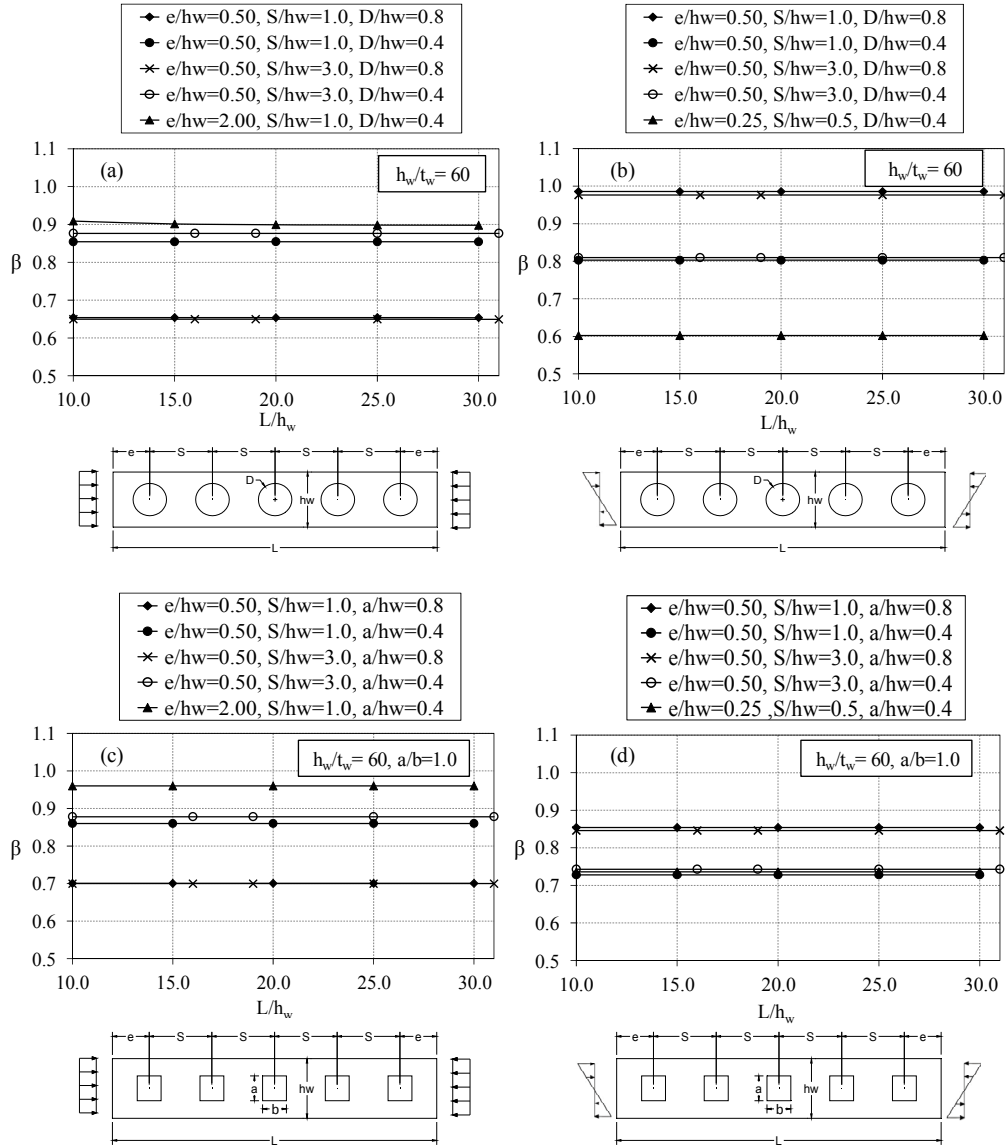


Fig. 5 Variation of buckling stress modification factor (β -factor) versus plate aspect ratio (L/h_w), for plates with circular or square openings under: (a) & (c) uniform compression; and (b) & (d) pure bending

opening size. It is worth noting that $e_{Limit-1}$ increases by increasing the opening spacing, where it reaches $0.55h_w$, $0.6h_w$ and $0.7h_w$ at spacing of $1.0h_w$, $2.0h_w$ and $3.0h_w$, respectively. At end distance that is in the range between $e_{Limit-1}$ and a second limiting value ($e_{Limit-2}$), and with opening size greater than $0.5h_w$, the plate longitudinal strips above and below the openings suffer buckling (as shown in Fig. 11(b)). It is worth noting that buckling takes place at a stress value greater than that at the solid plate buckling. That is why β -factor is greater than 1.0. Contrarily, $e_{Limit-2}$ decreases by increasing the opening spacing, where it reaches $1.75h_w$, $1.5h_w$ and $1.0h_w$ at spacing of $1.0h_w$, $2.0h_w$ and $3.0h_w$, respectively. With opening size less than or equal to $0.5h_w$, the end strip suffers buckling,

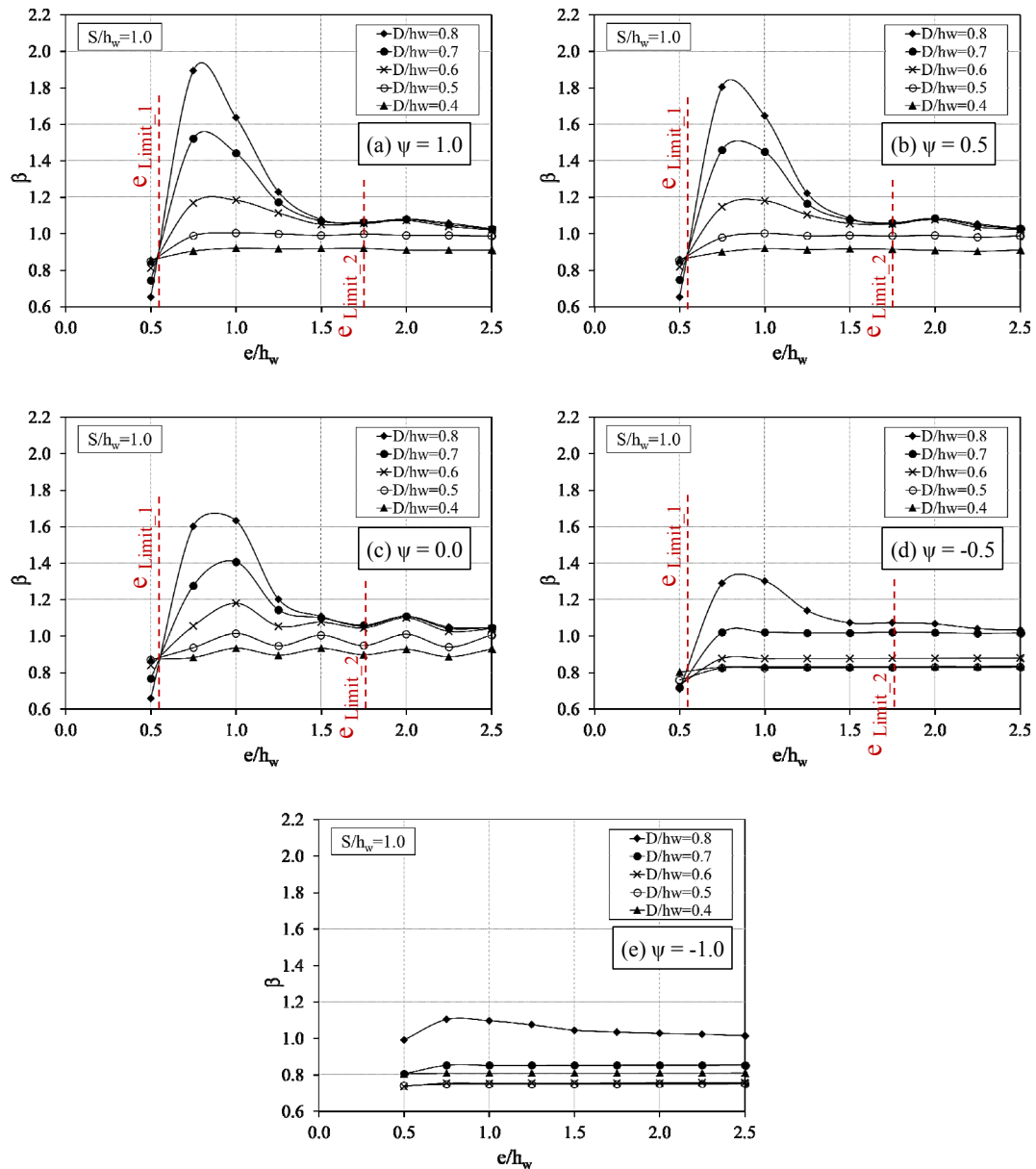


Fig. 6 Variation of buckling stress modification factor (β -factor) versus e/h_w and D/h_w for $S/h_w = 1.0$, in case of circular openings under different loading patterns

and the buckling behavior becomes less sensitive to the change in the opening end distance and spacing. At end distance greater than or equal to $e_{Limit-2}$, β -factor is independent of the opening end distance and spacing. Meanwhile, the plate end strip suffers buckling at a stress value close to that of solid plate buckling, where the end strip width allows a buckling wave to form similar to that of the solid plate buckling (as shown in Fig. 11(a2)).

For web plate with openings subject to loading pattern of ψ equal to -0.5, a behavior almost

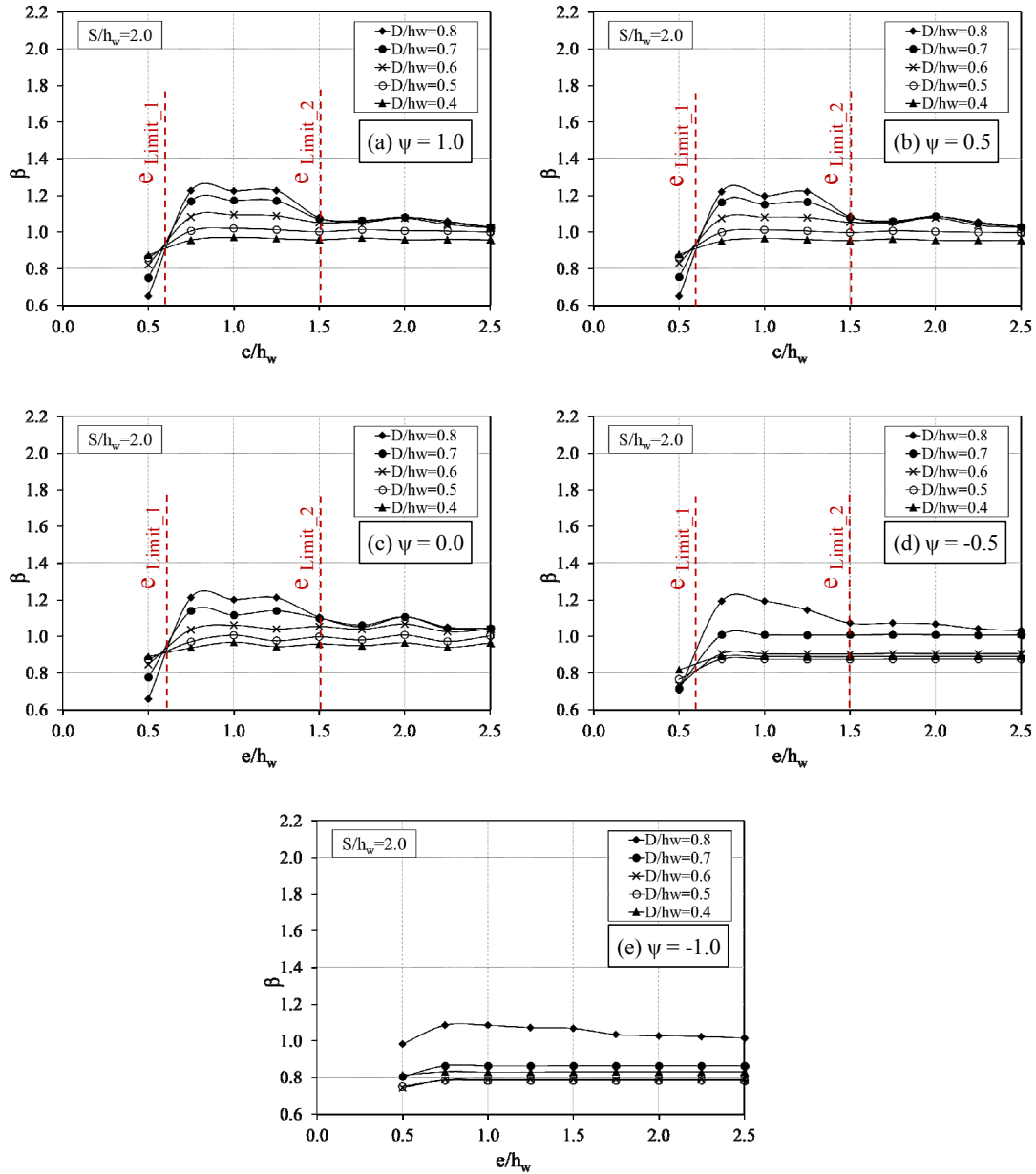


Fig. 7 Variation of buckling stress modification factor (β -factor) versus e/h_w and D/h_w for $S/h_w = 2.0$, in case of circular openings under different loading patterns

similar to that under compression loading is revealed. However, at end distance that is in the range between $e_{Limit-1}$ and $e_{Limit-2}$, an opening size of more than or equal to $0.7h_w$ is controlling the effect of end distance on β -factor, rather than $0.5h_w$ as detected in the case of compression loading. Furthermore, For web plate with openings subject to pure bending with loading pattern of ψ equal to -1.0 , the longitudinal strip under compression suffers buckling at a stress value less than that at the end or post strips buckling. Accordingly, β -factor in almost independent of the opening end

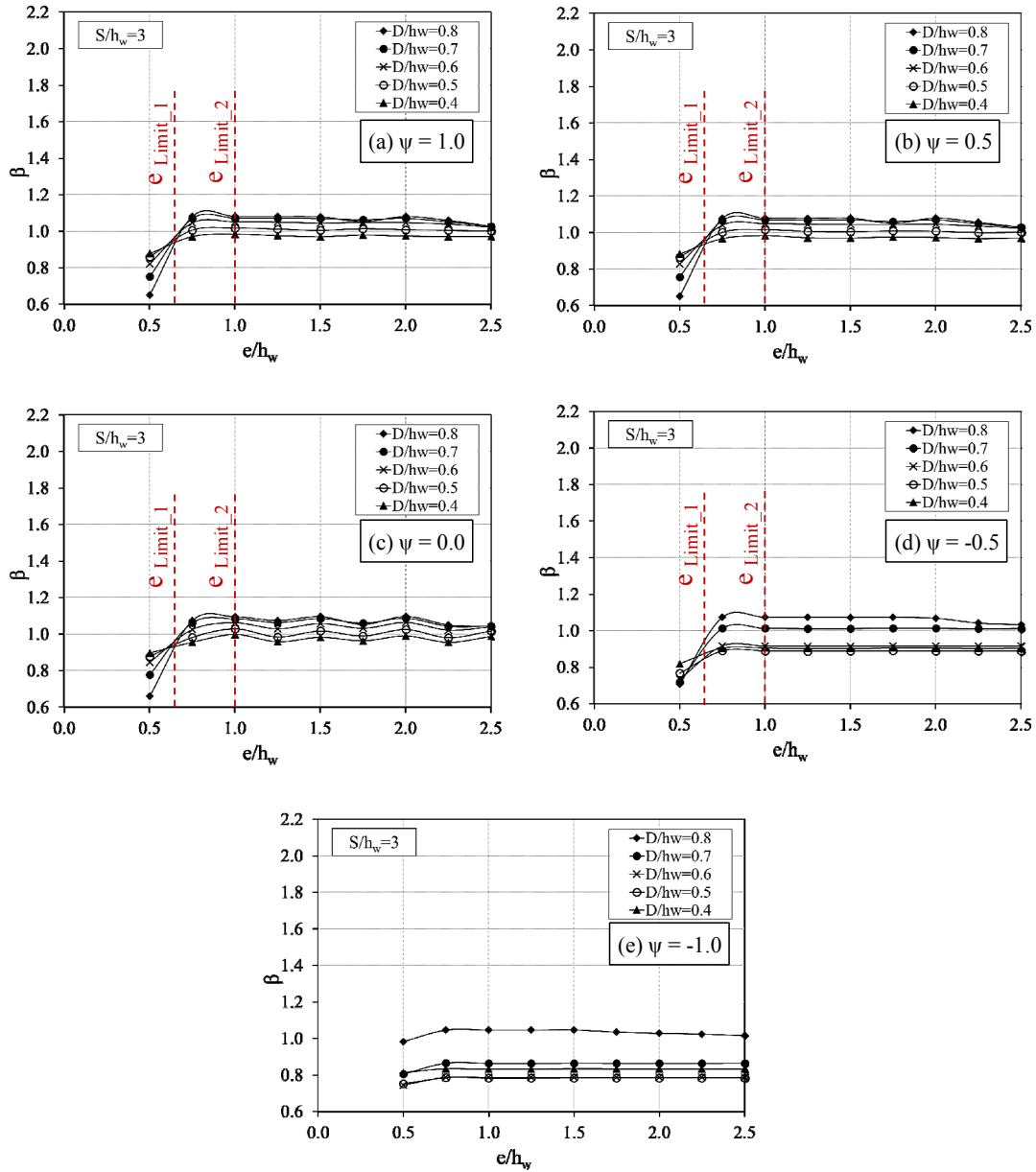


Fig. 8 Variation of buckling stress modification factor (β -factor) versus e/h_w and D/h_w for $S/h_w = 3.0$, in case of circular openings under different loading patterns

distance. An exception is evident when the opening size is equal to $0.8h_w$, where a behavior similar to that under compression loading is revealed with a limited effect of end distance.

It is evident that web plates under combined compression and tension loading ($\psi = -0.5$ and -1.0) are less sensitive to the change in opening end distance compared with those under compression loading ($\psi = 1.0, 0.5$, and 0.0). In addition, the lowest value of β -factor has been observed at the smallest value of e considered for the opening end distance ($e = 0.5h_w$), at all loading patterns. In the

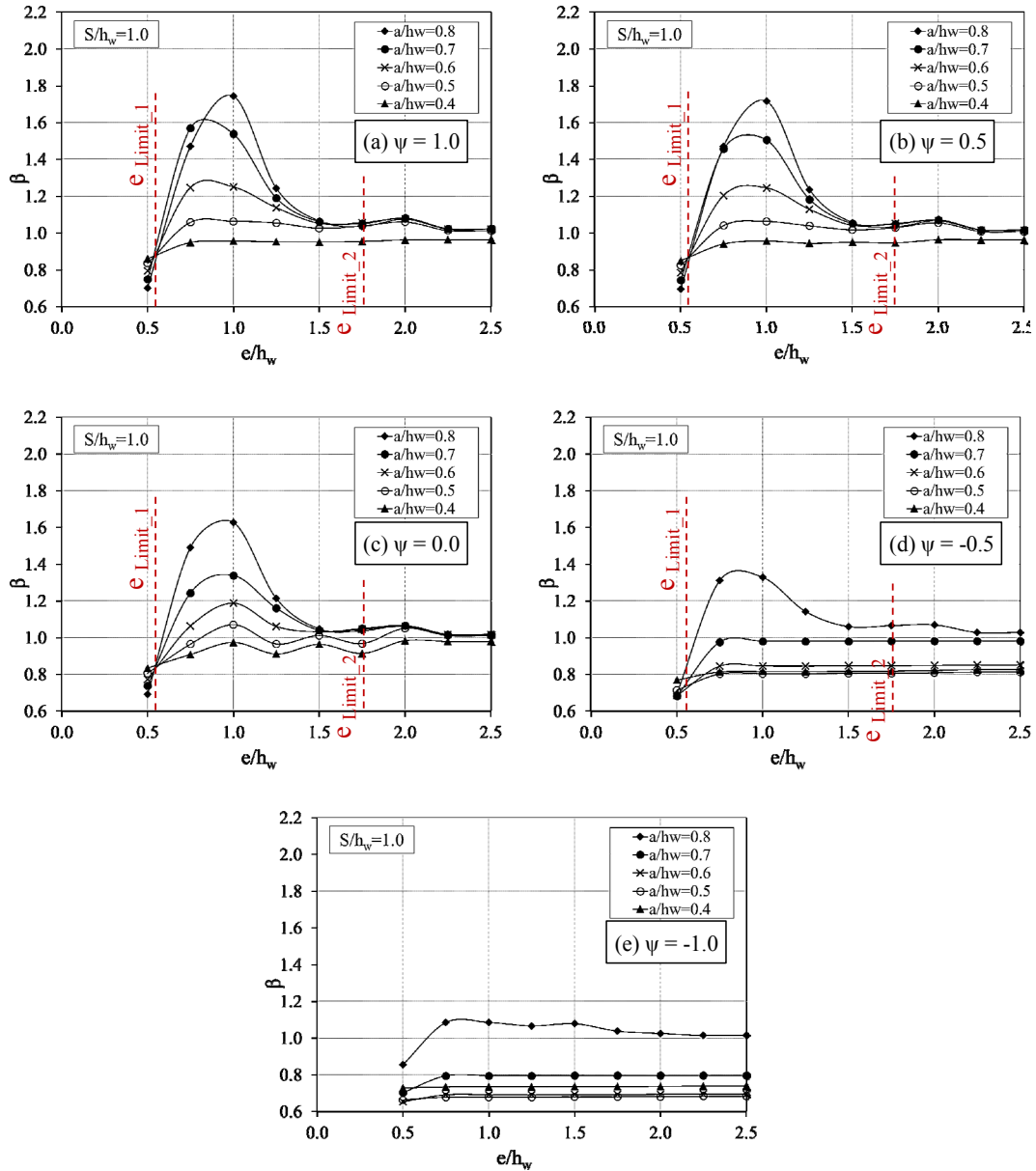


Fig. 9 Variation of buckling stress modification factor (β -factor) versus e/h_w and a/h_w for $S/h_w = 1.0$, in case of square openings under different loading patterns

end distance range of $e_{Limit-2}$ to $2.5h_w$, the β -factor becomes almost independent of the opening end distance and spacing, approaching 1.0 for plates under compression loading ($\psi = 1.0, 0.5$, and 0.0) and approaching a range of 0.7 to 1.0 for plates under both compression and tension loadings ($\psi = -0.5$ and -1.0). It is also evident that β -factor is directly proportional to the opening size.

The effect of opening spacing (S) is sound when comparing Figs. 6-8, for circular openings, and Figs. 9-10 for square openings. Based on the full spectrum of the obtained results (Hamed *et*

al. 2015), spacing less than or equal to $2.0h_w$ has been classified as small spacing; meanwhile, spacing greater than $2.0h_w$ has been classified as large spacing. At a small opening spacing (example is $S = h_w$), the end distance has significant effect on β -factor. On the other hand, at a larger opening spacing (example is $S = 3.0h_w$), the end distance has almost no effect on β -factor, at all loading patterns. Hence, for large opening spacing the opening size emerges as the controlling parameter for β -factor. This is attributed to the observed buckling at the plate post strip when

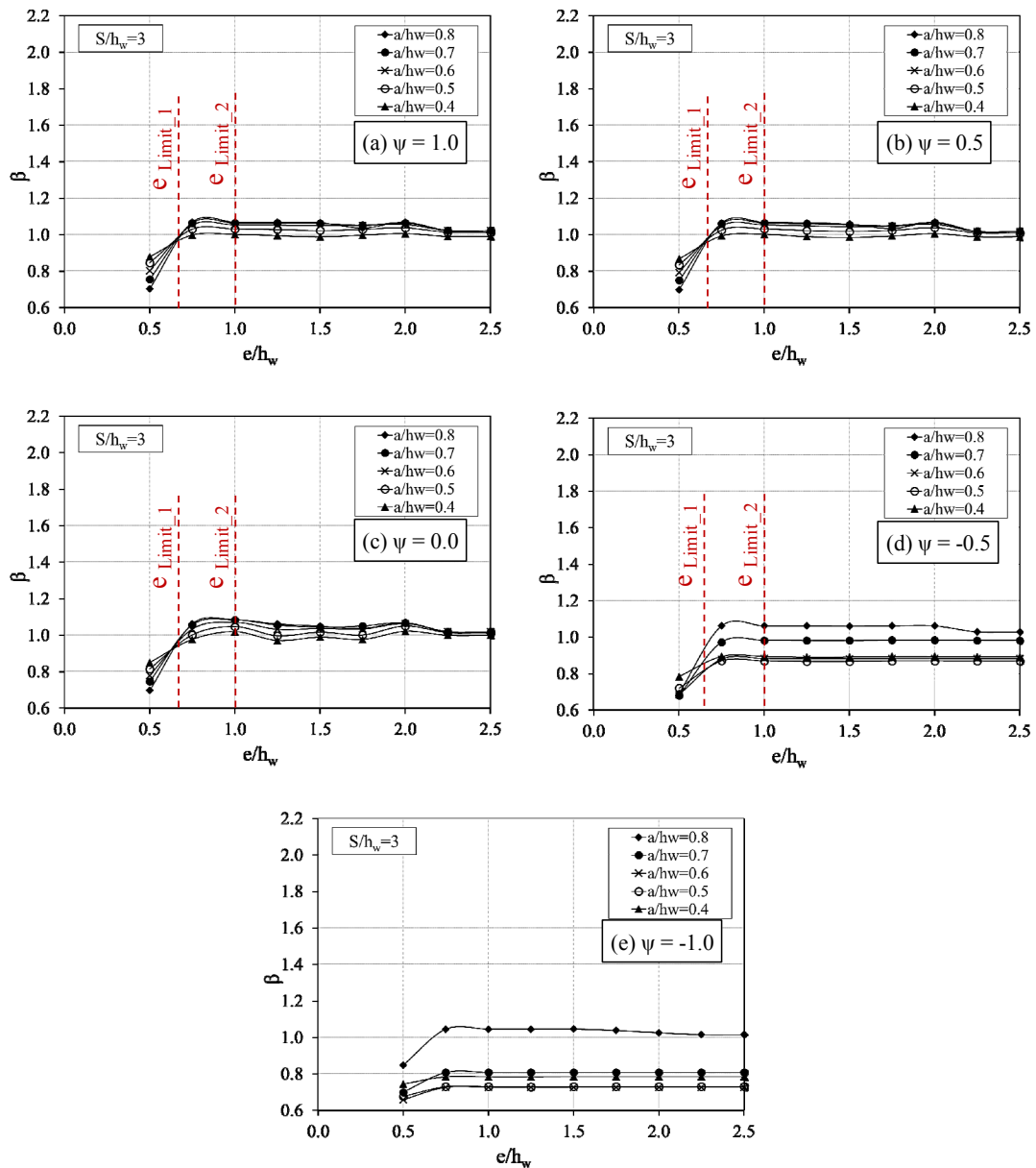


Fig. 10 Variation of buckling stress modification factor (β -factor) versus e/h_w and a/h_w for $S/h_w = 3.0$, in case of square openings under different loading patterns

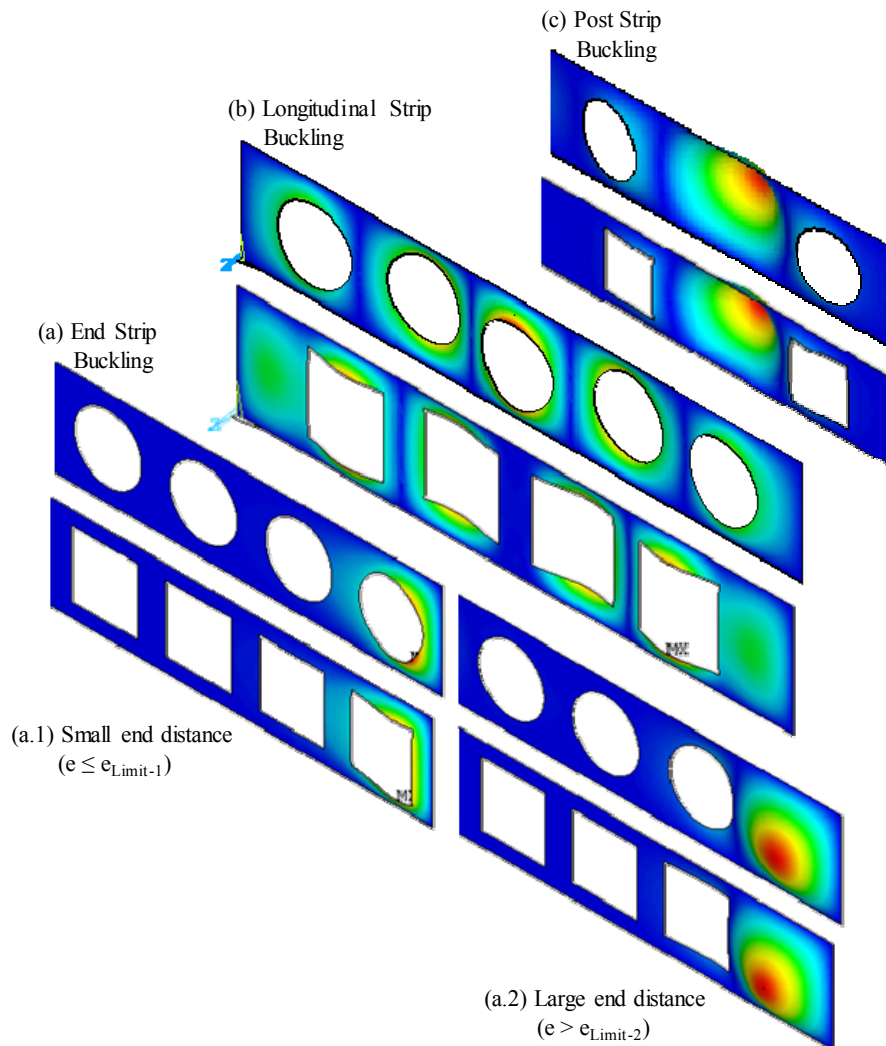


Fig. 11 Observed buckling modes at: (a) End strip; (b) Longitudinal strip; and (c) Post strip

opening spacing is increased, where the end distance becomes ineffective (as shown in Fig. 11(c)).

Fig. 12 illustrates the variation of β -factor versus rectangular opening size (a) at different opening aspect ratios ($a/b = 0.5, 1.0$ and 2.0). The opening end distance and spacing have been set equal to $1.0h_w$ in order to avoid the plate end and post strips buckling. Consequently, buckling occurs in the plate longitudinal strips. Furthermore, at these values of opening end distance and spacing, the opening size has a sound effect on buckling behavior as previously reported. In general, it is evident that β -factor increases with increasing opening aspect ratio (a/b), at all cases of loading patterns. However, the superior behavior of the aspect ratio ($a/b = 2.0$) is maintained until an opening size limit at which the aspect ratio of ($a/b = 1.0$) precedes. The opening size limit is varied between $0.6h_w$ and $0.8h_w$ based on the applied loading pattern. This behavior is attributed to the positive/negative effect of opening aspect ratio along with the associated opening size on the slenderness ratio (width/thickness) of the plate longitudinal strip. The resulted slenderness ratio, in

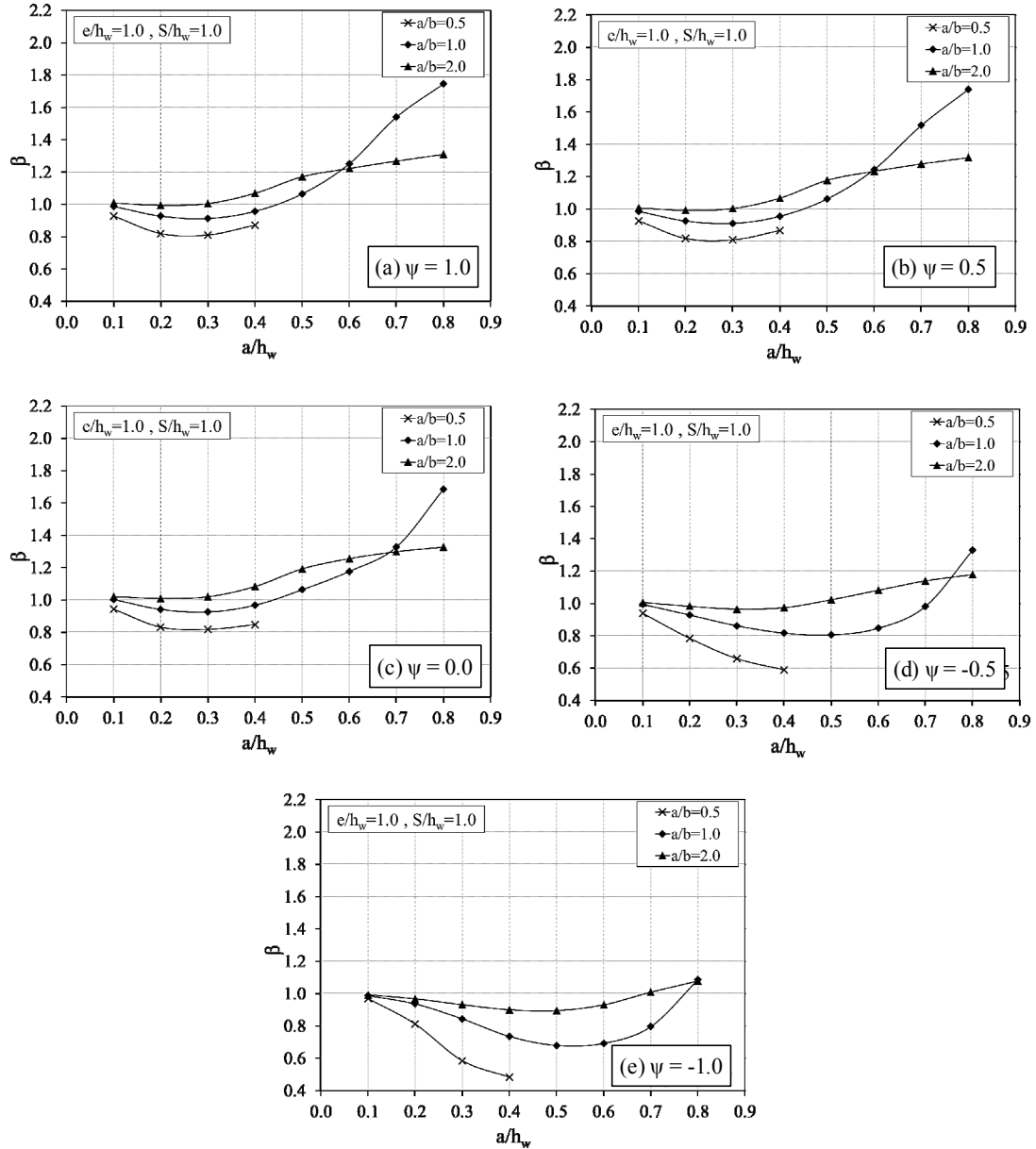


Fig. 12 Variation of buckling stress modification factor (β -factor) with a/h_w for $e/h_w = 1.0$, $S/h_w = 1.0$ and various values of opening aspect ratio (a/b), under different loading patterns

turn, affects the resulted buckling stress and β -factor. For example, at rectangular opening aspect ratio of ($a/b = 2.0$) with large opening size ($a > 0.3h_w$ for $\psi = 1.0, 0.5, 0.0$; $a > 0.5h_w$ for $\psi = -0.5$; and $a > 0.7h_w$ for $\psi = -1.0$) the plate longitudinal strip has low slenderness ratio and consequently the resulted β -factor is greater than 1.0. Furthermore, at rectangular opening aspect ratio of ($a/b = 0.5$), with all opening sizes the plate longitudinal strip has high slenderness ratio and consequently the resulted β -factor is less than 1.0.

Regression analysis has been performed for the obtained FE results of web plates with circular and square openings (with R-square greater than 0.98). Equations have been proposed for $e_{\text{Limit-1}}$, $e_{\text{Limit-2}}$, and β -factor in line with the aforementioned observations. The limits $e_{\text{Limit-1}}$ and $e_{\text{Limit-2}}$ can be expressed as $[e_{\text{Limit-1}} = 0.47h_w + 0.075S]$ and $[e_{\text{Limit-2}} = 2.16h_w - 0.375S]$. For compression loading ($\psi = 1.0, 0.5,$ and 0.0) with opening size that is less than or equal to $0.5h_w$, β -factor can be expressed as $[\beta\text{-factor} = 0.5 + 1.6 (e-D/2)/h_w]$ for $e \leq e_{\text{Limit-1}}$, and $[\beta\text{-factor} = 0.9 + 0.01 (e-D/2)/h_w]$ for $e > e_{\text{Limit-1}}$. With opening size that is greater than $0.5h_w$, β -factor can be expressed as $[\beta\text{-factor} = 0.5 + 1.6 (e-D/2)/h_w]$ for $e \leq e_{\text{Limit-1}}$, and $[\beta\text{-factor} \geq 1.0]$ for $e > e_{\text{Limit-1}}$. For combined compression and tension loading ($\psi = -0.5$ and -1.0) with opening size that is less than or equal to $0.7h_w$, β -factor can be expressed as $[\beta\text{-factor} = 0.6 + 0.7 (e-D/2)/h_w]$ for $e \leq e_{\text{Limit-1}}$, and $[\beta\text{-factor} = 0.8 + 0.05 (e-D/2)/h_w]$ for $e > e_{\text{Limit-1}}$. With opening size that is greater than $0.7h_w$, β -factor can be expressed as $[\beta\text{-factor} = 0.5 + 1.6 (e-D/2)/h_w]$ for $e \leq e_{\text{Limit-1}}$, and $[\beta\text{-factor} \geq 1.0]$ for $e > e_{\text{Limit-1}}$. It is worth noting that the circular opening size “ D ” can be replaced in the aforementioned equations with “ a ” for the square opening.

Based on the obtained results of elastic buckling analyses and within the range of the studied parameters and loading patterns, it is recommended to locate the first opening in a web plate at an end distance of $1.0h_w$ and within openings spacing of $1.0h_w$. Hence, an opening size greater than or equal to $0.5h_w$ is also recommended for circular or square openings. For non-square openings, rectangularity ratio of a/b greater than 1.0 is recommended in association with an opening size that is less than or equal to $0.6h_w$. For a loading pattern of pure bending, the opening size is particularly recommended to be greater than or equal to $0.7h_w$.

4.2 Inelastic buckling

Figs. 13(a) and (b) illustrate the variation of critical buckling stress (σ_{cr}/σ_y) versus plate aspect ratio (L/h_w) for various values of opening size (“ D ” for circular opening in Fig. 13a, or “ a ” for square opening in Fig. 13(b)) and plate slenderness ratio (h_w/t_w). The opening end distance (e) and spacing (S) are kept constant and equal to $1.0h_w$. The behavior has been depicted under uniform compression. It is worth noting that the effect of other loading patterns on inelastic buckling of web plates with openings is considered beyond the scope of this study. It is evident that the plate aspect ratio has no effect on the inelastic buckling load of web plates with openings. It is also evident that the critical buckling stress decreases with increasing plate slenderness (h_w/t_w) at small opening size (“ D ” or “ a ” equals $0.4h_w$). Meanwhile, for large opening size (“ D ” or “ a ” equals $0.8h_w$) the change in plate slenderness does not affect the resulted buckling stress.

Figs. 13(c) and (d) illustrate the variation of critical buckling stress (σ_{cr}/σ_y) versus opening end distance for various values of opening size (“ D ” for circular opening in Fig. 13(c), or “ a ” for square opening in Fig. 13(d)) and plate slenderness ratio (h_w/t_w). The opening spacing (S) and plate aspect ratio (L/h_w) are kept constant and equal to $1.0h_w$ and 10, respectively. The behavior has been depicted under uniform compression. It is evident that the critical buckling stress is constant for all the range of end distance, when the opening size is small (“ D ” or “ a ” equals $0.4h_w$). Meanwhile, for large opening size (“ D ” or “ a ” equals $0.8h_w$) the critical buckling stress becomes minimal at end distance of $0.5h_w$ then it increases with convergence to a constant value at end distance of $1.0h_w$. This behavior is attributed to the fact that the end strip width decreases (width = $[e-D/2]$ for circular opening, or $[e-a/2]$ for square opening) with the small end distance and large opening size, leading to a lower buckling stress.

Figs. 14 and 15 show the variation of critical buckling stress (σ_{cr}/σ_y) versus plate slenderness

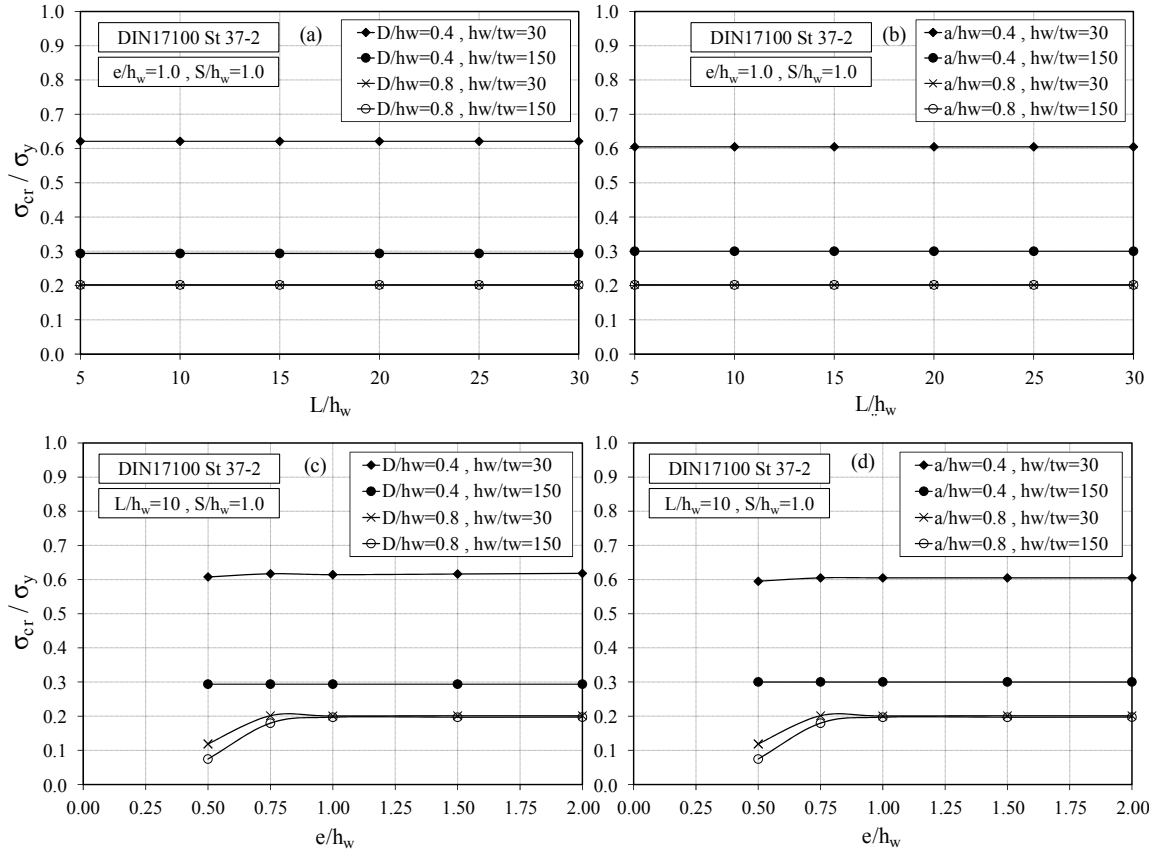


Fig. 13 Variation of critical buckling stress (σ_{cr}/σ_y) with (a) & (b) plate aspect ratio (L/h_w) and (c) & (d) opening normalized end distance (e/h_w), for different values of opening size and plate slenderness ratios under uniform compression

ratio (h_w/t_w) for different values of opening size ($0.4h_w$, $0.6h_w$ and $0.8h_w$), under both elastic and inelastic analyses. Two steel grades of DIN-17100 have been employed, namely: ST-37/2 and ST-52/3. The plate aspect ratio is kept constant and equal to 20; meanwhile, the opening end distance and spacing are also kept constant and equal to $1.0h_w$. The behavior has been depicted under uniform compression. It is evident that the critical buckling stress always decreases with increasing plate slenderness ratio. For low values of h_w/t_w (thick plates), the elastic buckling stress is higher than that of inelastic buckling; accordingly, the failure occurs due to material yielding. At particular slenderness ratio, which varies based on opening size and steel grade, the elastic buckling stress becomes lower than that of inelastic buckling. This indicates the change of failure mode from yielding to elastic buckling. The plate slenderness ratio at which the failure mode changes from yielding to elastic buckling increases with increasing the opening size. Hence, with large opening size (example: D or a is equal to $0.8h_w$), the yielding failure has been reported in association with all values of plate slenderness ratio (h_w/t_w from 30 to 150), with steel grade ST-37/2. Contrarily, the plate slenderness ratio at which the failure mode changes from yielding to elastic buckling decreases with increasing the steel yield strength. It is also evident that the inelastic post-buckling strength decreases with increasing the opening size.

Figs. 16(a) and (b) report the resulted plate critical slenderness ratio (at which the failure mode changes from yielding to elastic buckling) as a function of opening size for both steel grades (ST-37/2 and ST-52/3). The behavior has been depicted under uniform compression. The resulted values are associated with the range of studied parameters, elastic-perfect plastic material, perfect plates without imperfection, and neglecting the effect of residual stresses. Hence, at a particular

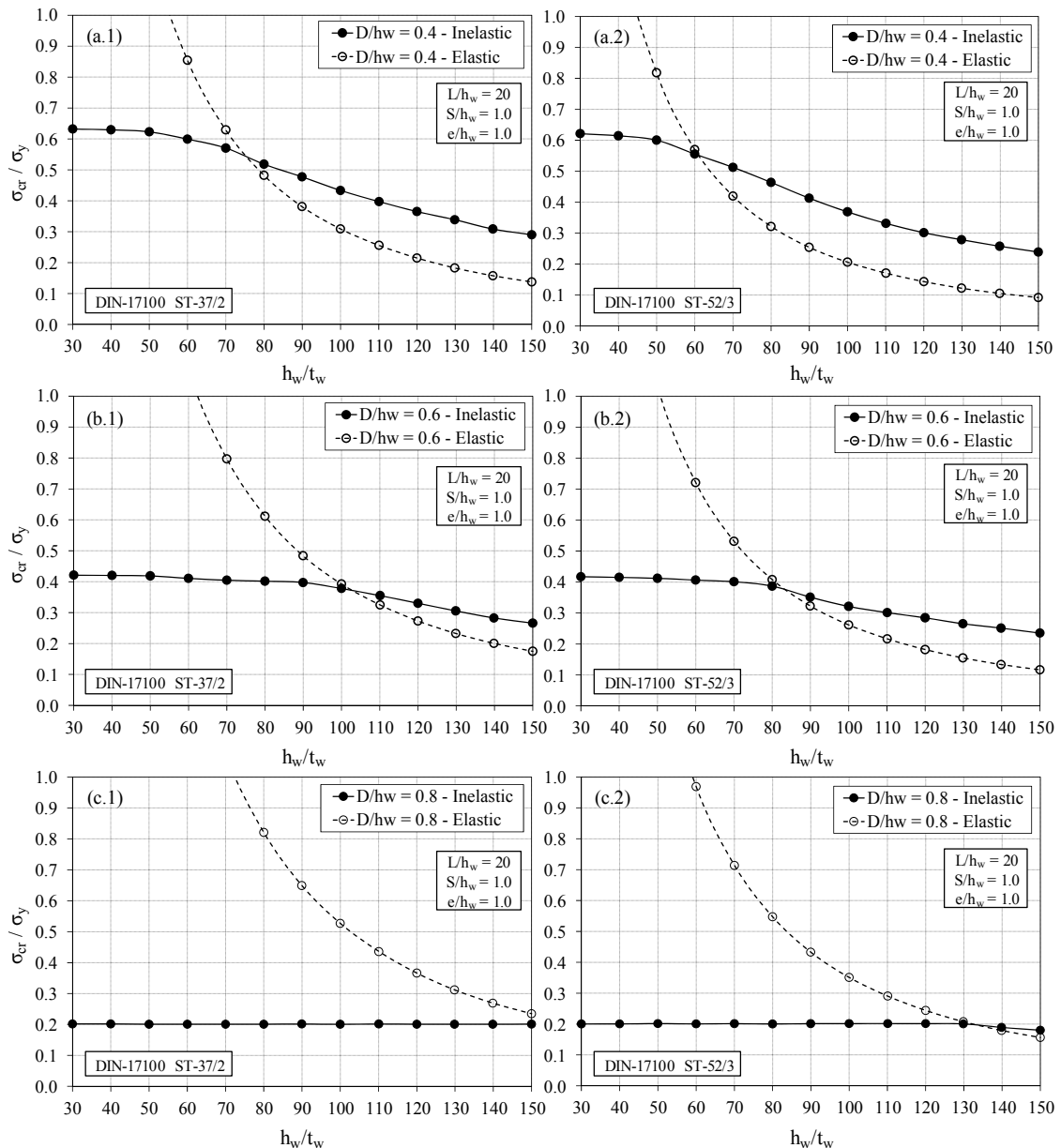


Fig. 14 Variation of critical buckling stress (σ_{cr}/σ_y) with plate slenderness ratio (h_w/t_w) for different circular opening sizes and steel grades within elastic and inelastic analyses under uniform compression: (a) $D/h_w = 0.4$; (b) $D/h_w = 0.6$; and (c) $D/h_w = 0.8$

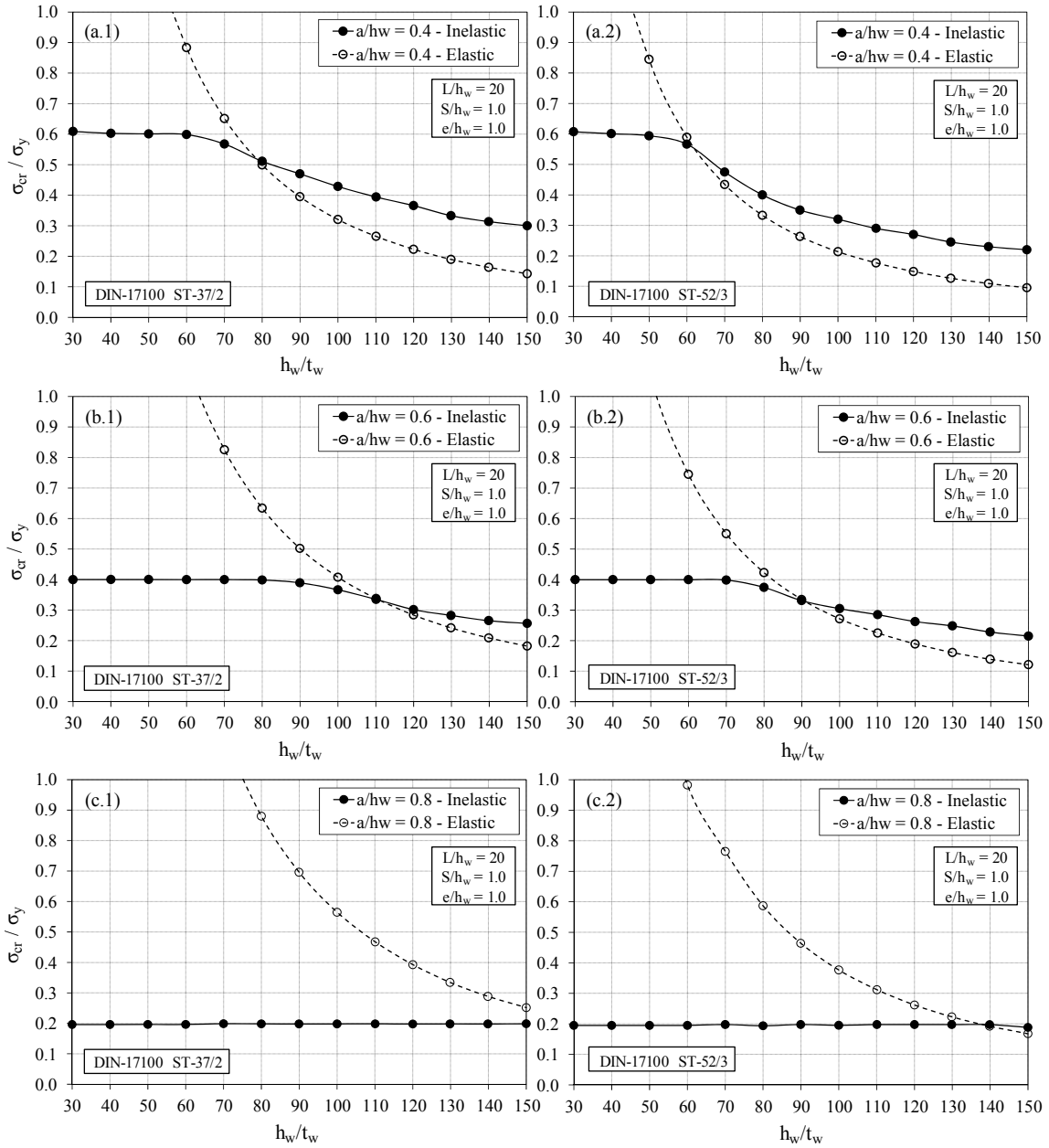


Fig. 15 Variation of critical buckling stress (σ_{cr}/σ_y) with plate slenderness ratio (h_w/t_w) for different square opening sizes and steel grades within elastic and inelastic analyses under uniform compression: (a) $a/h_w = 0.4$; (b) $a/h_w = 0.6$; and (c) $a/h_w = 0.8$

slenderness ratio (h_w/t_w), if the opening size is greater than the size revealed in these figures at a particular steel grade, yielding failure occur. Consequently, elastic buckling shall take place with smaller opening sizes. It is worth noting also that a web plate with openings having slenderness ratio lower than the critical ratio associated with the corresponding solid plate (associated with

D/h_w or $a/h_w = 0.0$) shall always be subject to yielding failure at all opening sizes. Furthermore, the following observations can be reported:

- For opening sizes less than or equal to $0.5h_w$, the critical slenderness ratio gently increases with increasing the opening size. Meanwhile, for opening sizes greater than $0.5h_w$, the critical slenderness ratio steeply increases with opening size increase.
- By increasing the slenderness ratio, the elastic buckling failure becomes more dominating within the studied range of opening sizes.
- The critical slenderness ratio for the same opening size is adversely related to the steel yield strength.

Based on the obtained results in Figs. 16(a) and (b), an expression has been developed for the critical slenderness ratio as a function of normalized opening size (D/h_w or a/h_w), steel yield strength (σ_y) and the previously defined β -factor. The expression has been developed based on the best regression (R-Square = 0.99) for the obtained results and is given as: $(h_w/t_w)_{\text{Critical}} = [(95/\sqrt{\sigma_y})(\sqrt{\beta/(1-D/h_w)^{0.45}})]$. The first term of the expression ($95/\sqrt{\sigma_y}$) represents the critical slenderness ratio

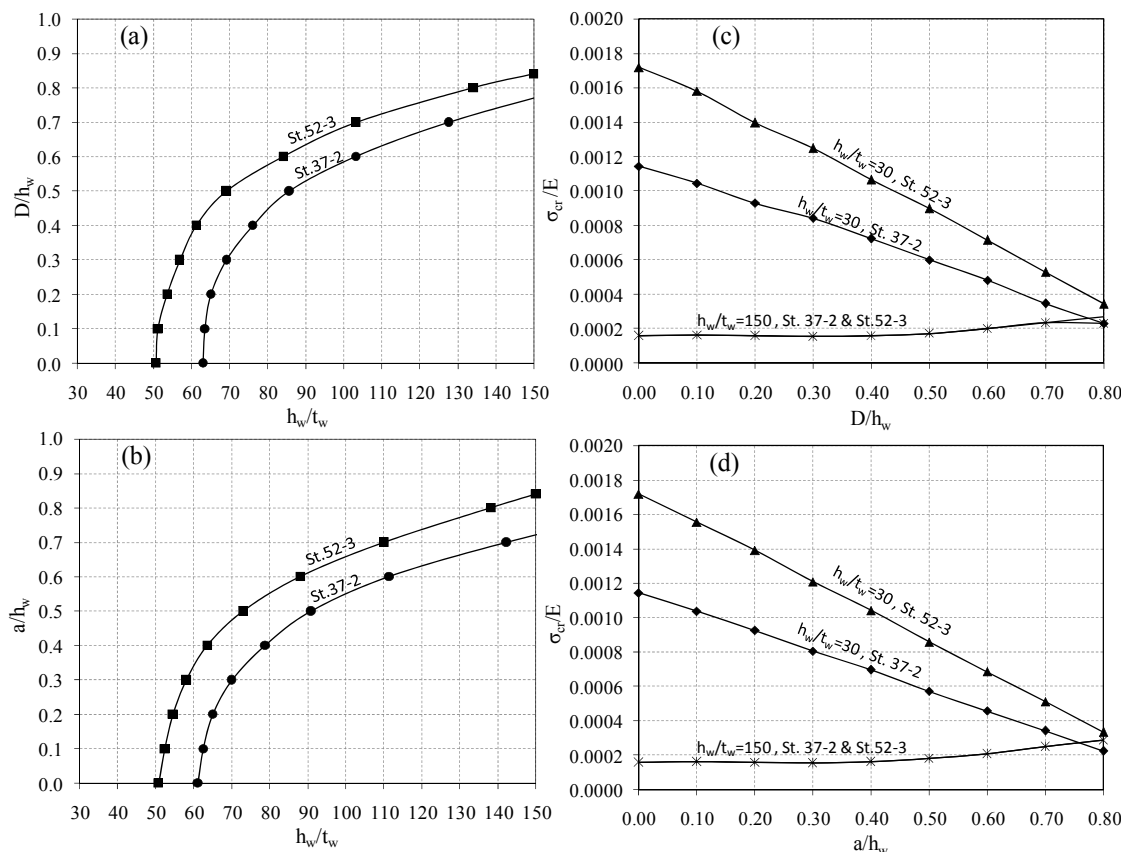


Fig. 16 A boundary between elastic and inelastic buckling for plates with: (a) circular openings; and (b) square openings, and the governing critical buckling stress versus opening size and steel grade for plates with: (c) circular openings; and (d) square openings, having slenderness ratios of 30 and 150

corresponding to the solid plate. Meanwhile, the second term of the expression $(\sqrt{\beta}/(1-D/h_w)^{0.45})$ represents the effect of openings as introduced in the plate. Furthermore, in order to consider the effect of residual stresses and initial imperfection, a reduction factor can be multiplied by this expression. The reduction factor varies between different design codes from 0.6 to 0.9. In the Egyptian code ECP-205 (2001), the adopted reduction factor for plates under compression is 0.74, and the expression is then given as $[(70/\sqrt{\sigma_y}) (\sqrt{\beta}/(1-D/h_w)^{0.45})]$.

Figs. 16(c) and (d) illustrate the variation of critical buckling stress versus opening size at the upper and lower boundaries of the studied plate slenderness ratios ($h_w/t_w = 150$ and $h_w/t_w = 30$) with both steel grades (ST-37/2 and ST-52/3). The behavior has been depicted under uniform compression. The reported critical buckling stress is the least of both elastic and inelastic buckling stresses. It is evident that for thin plates, having large value of h_w/t_w , the steel grade does not affect the critical buckling stress. This is attributed to the reported observation in Figs. 16(a) and (b), where at large slenderness ratio the elastic buckling stress is dominating for most of opening sizes, which is in turn independent of the yield stress. Contrarily for thick plates, having small value of h_w/t_w , the failure is always governed by steel yielding. Hence, the reported critical buckling stress is proportionally variant with the steel grade, and adversely variant with the opening size, as shown in the figures.

4.3 Initial imperfection

In the previously presented analysis, the plate was assumed almost perfect (having very small imperfection that is equal to $h_w/10,000$ for the nonlinear analysis). However, in practice, plate imperfection may occur due to fabrication, handling and erection processes. Hence, Figs. 17(a) and (b) have been dedicated to report the relationship between the induced plate stress, normalized to the yield stress, versus out of plane deformation at the critical point, for different values of plate bow (imperfection) and at plate opening sizes of $0.4h_w$ and $0.8h_w$, respectively. The behavior has been depicted under uniform compression. Four different magnitudes of plate imperfection have been considered in the study, namely: $h_w/10,000$ (representing perfect plate), $h_w/200$, $h_w/150$, and $h_w/100$. Accordingly, the following observations can be reported:

- The ultimate stress is reduced about 3%, 6.5% and 12% in association with a plate bow of $h_w/200$, $h_w/150$, and $h_w/100$, respectively.
- Fig. 17(a2) represents an enlargement for the elastic buckling zone in Fig. 17(a1). The resulted elastic buckling stress is equal to $0.094\sigma_y$, $0.066\sigma_y$, $0.060\sigma_y$, and $0.056\sigma_y$ in association with perfect plate and plates with bow of $h_w/200$, $h_w/150$, and $h_w/100$, respectively. Hence, the stress reduction is equal to 30%, 36% and 40% for plates with bow of $h_w/200$, $h_w/150$, and $h_w/100$, respectively, compared with the perfect plate.
- When the opening size is increased to $0.8h_w$ (as shown in Fig. 17(b)), the post-buckling load carrying capacity is reduced compared with that reported with opening size of $0.4h_w$ (as shown in Fig. 17(a)). This is attributed to the reduced section area with the larger opening size.

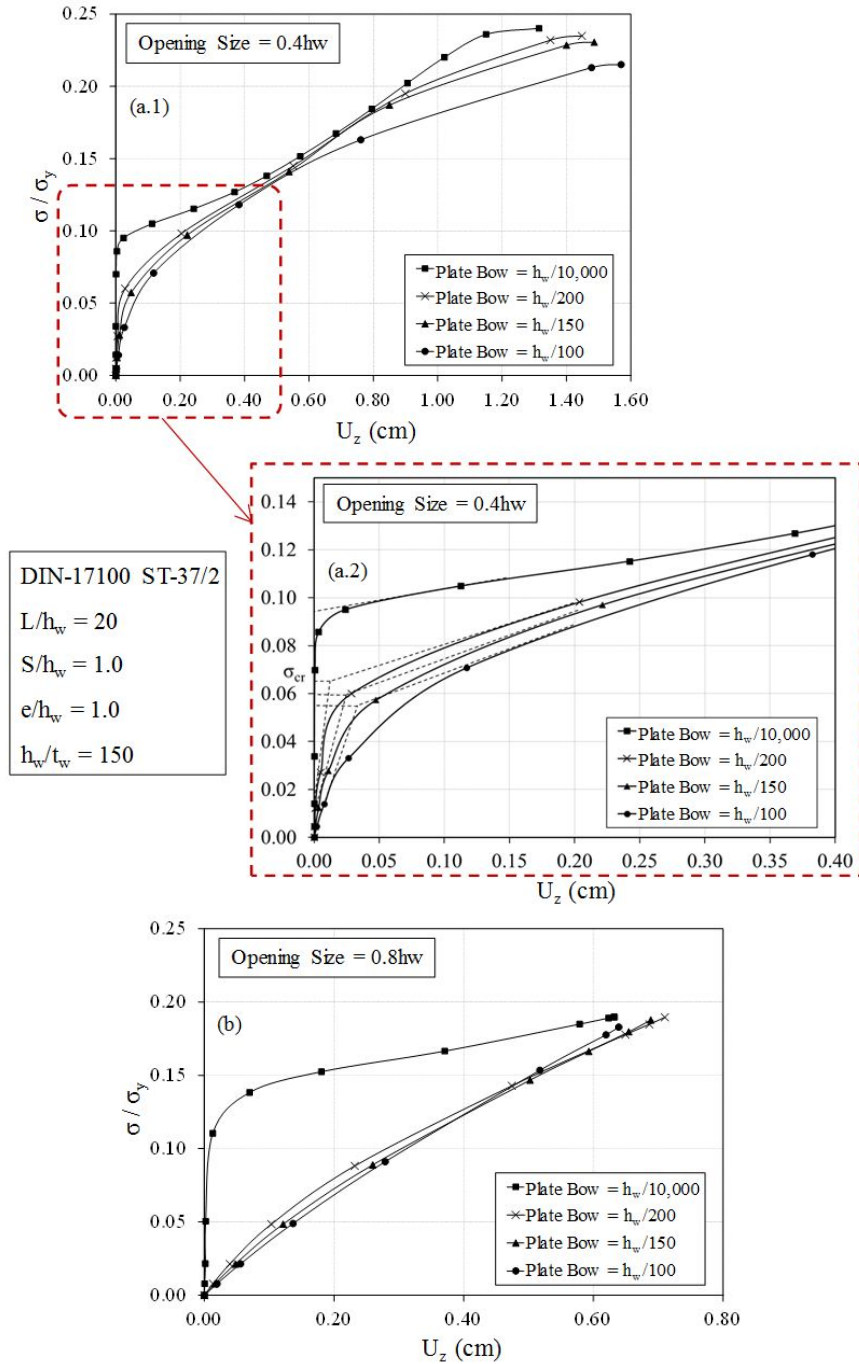


Fig. 17 Plate stress versus out of plane deformation for different values of plate bow (imperfection), where opening size is equal to: (a) $0.4h_w$; and (b) $0.8h_w$

5. Conclusions

In this study, the effect of different parameters on both elastic and inelastic critical buckling stresses has been investigated for steel web plates with openings. The parameters in question are plate aspect ratio; opening shape (circular or rectangular); end distance to first opening; opening spacing; opening size; plate slenderness ratio; steel grade; and initial web imperfection. The web plates are subject to in plane linearly varying compression with different loading patterns, ranging from uniform compression to pure bending. The web/flange interaction has been simplified by web edge restraints representing simply supported boundary conditions. Both linear and nonlinear finite element analyses have been performed, where results have been verified against those in the literature.

The general conclusions, within the range of studied models and parameters for both elastic and inelastic buckling, can be summarized as follows:

- (1) The plate with circular openings has almost the same behavior pattern of that with square openings, for all parameters and loading conditions.
- (2) The plate aspect ratio has no effect on the critical buckling stress.
- (3) The plate slenderness ratio is adversely proportional to the critical buckling stress.
- (4) The plate initial imperfection adversely affects both the critical buckling stress and the post-buckling strength.

The main conclusions for elastic buckling analysis can be summarized as follows:

- (1) The plate subject to compression is more sensitive to the change in different parameters compared with that subject to both compression and tension.
- (2) The plate with an opening size greater than $0.5h_w$ is recommended for circular or square openings. For non-square openings, a rectangularity ratio (in the plate depth direction) greater than 1.0 is recommended in association with an opening size that is less than or equal to $0.6h_w$. For a loading pattern of pure bending, the opening size is particularly recommended to be greater than or equal to $0.7h_w$.
- (3) The small values of end distance should be avoided. Plates with large values of end distance or plates with widely spaced openings have a critical buckling stress that is close to ($\geq 90\%$) that of the corresponding solid plate, when subjected to compression. Under combined compression and tension loading, however, a stress reduction of almost 30% is anticipated. Hence, the recommended values for opening end distance and spacing is $1.0h_w$.

The main conclusions for inelastic buckling analysis can be summarized as follows:

- (1) The critical buckling stress is constant for all the range of the opening end distance, when the opening size is small. Meanwhile, for large opening size it is recommended to have the end distance greater than or equal to $1.0h_w$.
- (2) The critical buckling stress is adversely proportional to the opening size.
- (3) The plate slenderness ratio at which the failure mode changes from yielding to elastic buckling increases with increasing the opening size. Meanwhile, it decreases with increasing the steel yield strength.
- (4) The plate with large slenderness ratio is subject to a dominating elastic buckling in

association with most of the opening sizes, which in turn is independent of the steel grade. Contrarily, the plate with small slenderness ratio is subject to failure that is always governed by steel yielding and opening size.

References

- AASHTO LRFD (1994), Bridge Design Specifications, Washington, D.C., USA.
- Anghel, V., Sorohan, S., Constantin, N., Gavan, M. and Boritu, A. (2011), "Numerical study of the lateral buckling of thin walled open cross-section beams", *SISOM 2011 and Session of Comission of Acoustics*, pp. 3-7.
- AWS-D1.1 (2004), Structural Welding Code – Steel; American Welding Society, 550 N.W. Le Jeune Road, Miami, FL, USA.
- ANSYS (1998), Swanson analysis system; release 11.0. Houston, LA, USA.
- Bruneau, M., Uang, C.M. and Sabelli, S.E. (1998), "Ductile Design of Steel Structures", McGraw Hill, New York, NY, USA.
- Chung, K.F., Liu, T.C.H. and Ko, C.H. (2001), "Investigation on vierendeel mechanism in steel beams with circular web openings", *J. Constr. Steel Res.*, **57**(5), 467-490.
- Durif, S., Bouchaïr, A. and Vassart, O. (2014), "Experimental and numerical investigation on web-post specimen from cellular beams with sinusoidal openings", *Eng. Struct.*, **59**, 587-598.
- ECP-205 (ASD) (2011), Egyptian Code of Practice for Steel Construction and Bridges; Housing and Research Center, Giza, Egypt.
- Ellobody, E. (2012), "Nonlinear analysis of cellular steel beams under combined buckling modes", *Thin-Wall. Struct.*, **52**, 66-79.
- El-Sawy, K.M. and Nazmy, A.S. (2001), "Effect of aspect ratio on the elastic buckling of uniaxially loaded plates with eccentric holes", *Thin-Wall. Struct.*, **39**(12), 983-998.
- El-Sawy, K.M., Nazmy, A.S. and Martini, M.I. (2004), "Elasto-plastic buckling of perforated plates under uniaxial compression", *Thin-Wall. Struct.*, **42**(8), 1083-1101.
- El-Sawy, K.M., Sweedan, A.M.I. and Martini, M.I. (2009), "Major-axis elastic buckling of axially loaded castellated steel columns", *Thin-Wall. Struct.*, **47**(11), 1295-1304.
- Erdal, F., Doan, E. and Saka, M.P. (2011), "Optimum design of cellular beams using harmony search and particle swarm optimizers", *J. Constr. Steel Res.*, **67**(2), 237-247.
- Hamed, A.N., Serror, M.H. and Mourad, S.A. (2015), "Critical buckling stress of castellated web plates under linearly varying uniaxial compression", M.Sc. Thesis; Department of Structural Engineering, Faculty of Engineering, Cairo University, Cairo, Egypt.
- Kamble, S.R. (2012), "Analysis of stress distribution in castellated beam using finite element method and experimental techniques", *Int. J. Mech. Eng. Appl. Res.*, **3**(3), 190-197.
- Kang, J. (2014), "Exact solutions of stresses, strains, and displacements of a perforated rectangular plate by a central circular hole subjected to linearly varying in-plane normal stresses on two opposite edges", *Int. J. Mech. Sci.*, **84**, 18-24.
- Komur, M.A. and Sonmez, M. (2008), "Elastic buckling of rectangular plates under linearly varying in-plane normal load with a circular cutout", *Mech. Res. Commun.*, **35**(6), 361-371.
- Maiorana, E., Pellegrino, C. and Modena, C. (2009), "Elastic stability of plates with circular and rectangular holes subjected to axial compression and bending moment", *Thin-Wall. Struct.*, **47**(3), 241-255.
- Moen, C.D. and Schafer, B.W. (2009), "Elastic buckling of thin plates with holes in compression or bending", *Thin-Wall. Struct.*, **47**(12), 1597-1607.
- Narayanan, R. and Chow, F.Y. (1984), "Ultimate capacity of uniaxially compressed perforated plates", *Thin-Wall. Struct.*, **2**(3), 241-264.
- Panedpojaman, P. and Rongram, T. (2014), "Design equations for vierendeel bending of steel beams with circular web openings", *Proceedings of the World Congress on Engineering*, London, UK, July.

- Redwood, R., Zaarour, W. and Megharief, J. (1996), "Web post buckling in castellated beams", *Proceedings of International Conference on Advances in Steel Structures*, Hong Kong, December, pp. 67-71.
- Serror, M.H. (2011), "Effect of web opening on buckling instability of simply supported steel I-beam", *J. Civil Eng. Arch.*, **5**(9), 809-818.
- Shanmugam, N.E., Thevendran, V. and Tan, Y.H. (1999), "Design formula for axially compressed perforated plates", *Thin-Wall. Struct.*, **34**(1), 1-20.
- Shanmugam, N.E., Lian, V.T. and Thevendran, V. (2002), "Finite element modelling of plate girders with web openings", *Thin-Wall. Struct.*, **40**(5), 443-464.
- Soltani, M.R., Bouchaïr, A. and Mimoune, M. (2012), "Nonlinear FE analysis of the ultimate behavior of steel castellated beams", *J. Constr. Steel Res.*, **70**, 101-114.
- Sonck, D., Impe, R.V., Belis, J. and Vandebroek, M. (2011), "Buckling failure of compressed cellular members", *Proc. IABSE-IASS*.
- Sonck, D., Impe, R.V. and Belis, J. (2014), "Experimental investigation of residual stresses in steel cellular and castellated members", *Constr. Build. Mater.*, **54**, 512-519.
- Sweedan, A.M.I. and El-Sawy, K.M. (2011), "Elastic local buckling of perforated webs of steel cellular beamcolumn elements", *J. Constr. Steel Res.*, **67**(7), 1115-1127.
- Thomas, P. (1996), "Plate buckling analysis using linear and non-linear finite element methods", Youngstown State University, Youngstown, OH, USA.
- Timoshenko, S. and Gere, J. (1961), *Theory of Elastic Stability*, (2nd Ed.), New York, NY, USA.
- Tsavdaridis, K.D. and Mello, C.D. (2011), "Web buckling study of the behaviour and strength of perforated steel beams with different novel web opening shapes", *J. Constr. Steel Res.*, **67**(10), 1605-1620.
- Wakchaure, M.R., Sagade, A.V. and Auti, V.A. (2012), "Parametric study of castellated beam with varying depth of web opening", *Int. J. Sci. Res. Publ.*, **2**(8), 1-6.
- Wang, P., Ma, Q. and Wang, X. (2014), "Investigation on Vierendeel mechanism failure of castellated steel beams with fillet corner web openings", *Eng. Struct.*, **74**, 44-51.
- Yuan, W.B., Kim, B. and Li, L.Y. (2014), "Buckling of axially loaded castellated steel columns", *J. Constr. Steel Res.*, **92**, 40-45.